

Seafloor characterization in the southernmost Okinawa Trough from underwater optical imagery

Yu-Cheng Chou^{*}, Chau-Chang Wang, Hsin-Hung Chen, and Yuan-He Lin

Institute of Undersea Technology, National Sun Yat-sen University, Kaohsiung City, Taiwan

Article history:

Received 31 October 2018

Revised 4 March 2019

Accepted 14 March 2019

Keywords:

Southern Okinawa Trough, Seafloor imaging and sampling, ATIS, V-Corer, FITS, TVG

Citation:

Chou, Y.-C., C.-C. Wang, H.-H. Chen, and Y.-H. Lin, 2019: Seafloor characterization in the southernmost Okinawa Trough from underwater optical imagery. *Terr. Atmos. Ocean. Sci.*, 30, 717-737, doi: 10.3319/TAO.2019.03.14.01

ABSTRACT

This paper presents the seafloor survey results obtained in 2016 and 2017 using four deep-towed vehicles, developed by the Institute of Undersea Technology at National Sun Yat-sen University, for investigating mineral resource potential offshore northeastern Taiwan. The deep-towed vehicles include the Abyss Twist-pair Imaging System (ATIS), the Video-guided Multi-corer (V-Corer), the TV-guided Grabber (TVG), and the Fiber-optical Instrumentation Towed System (FITS). The seafloor video surveys and sampling were conducted at five survey sites in the southern Okinawa Trough through five survey cruises. A total of 82.69 km of seafloor survey tracks were accomplished and plenty of seafloor characteristics and ecological phenomena were observed through the four deep-towed vehicles. The seafloor survey results, including the video data and the samples of animals, sediments, and mounds, have been provided to different scientific teams for conducting research on marine geophysics, marine geology, marine geochemistry, and marine ecology. The video data can be cross-checked and used as the supporting evidence for the analysis results from the scientific researchers.

1. INTRODUCTION

Deep-sea metallic and industrial minerals are potential sources of primary supply in the future as the use of minerals has been increasing with the rapid growth of economic development in the world. In order to investigate mineral resources within the exclusive economic zone (EEZ) of Taiwan, the Central Geological Survey (CGS), an administrative agency under the Ministry of Economic Affairs (MOEA) of Taiwan, launched a 4-year program entitled “Geological Investigation of Mineral Resource Potential in the Offshore Northeastern Taiwan” in 2016. The 4-year CGS program consists of three projects, one of which is entitled “Geochemical Investigation and Sea Floor Imaging”, which aims to (1) understand the classifications, compositions, and spatial distribution of submarine hydrothermal deposits and altered minerals; (2) investigate the characteristics of hydrothermal alteration and mineralization; and (3) evaluate the types and potential of submarine mineral resources offshore northeastern Taiwan (Su 2016, 2017; Lin et al. 2019a, b).

Under the above project, a subproject entitled “Video Surveys and Sampling of Seafloor Mineral Deposits” is executed by the Institute of Undersea Technology (IUT) at National Sun Yat-sen University (NSYSU) (Wang 2016; Chen 2017). The subproject aims to apply deep-towed vehicles to seafloor imaging and sampling in order to collect visual observation data and different types of samples from the survey sites of interest. The visual observation data and samples collected from the seafloor are essential to fulfil the aforementioned objectives of the CGS project.

On the other hand, video survey with a deep-towed vehicle close to the seafloor is a detailed but small-scale survey method. Therefore, results from large-scale surveys are necessary to determine the areas of interest worth conducting detailed surveys and sampling. Under the 4-year CGS program, large-scale survey results, provided by “High-resolution Sonar and Magnetic Surveys” project (Hsu 2016, 2017; Doo et al. 2019; Tsai et al. 2019) and “Seismic and Heat Flow Surveys” project (Liu 2016, 2017; Hsu et al. 2019; Wu et al. 2019), are utilized to determine the sites of interest for small-scale video survey and sampling purposes. For the years of 2016 and 2017, the large-scale survey area was located at the

^{*} Corresponding author
E-mail: ychou@mail.nsysu.edu.tw

southern Okinawa Trough from E122°35' to E123°15' and from N24°47.32' to N25°30', with a depth range from 900 - 1800 m, as shown in Fig. 1. Based on the large-scale survey results obtained by the above two CGS projects, several survey sites were then chosen for small-scale seafloor video surveys and video-guided sampling conducted by the IUT.

In the years of 2016 and 2017, deep-towed vehicles developed by the IUT were utilized in multiple survey cruises for seafloor imaging and sampling around the sites of interest offshore northeastern Taiwan. The deep-towed vehicles include the Abyss Twist-pair Imaging System (ATIS), the Video-guided Multi-corer (V-Corer), the TV-guided Grabber (TVG), and the Fiber-optical Instrumentation Towed System (FITS). A total of 82.69 km of seafloor survey tracks were accomplished and plenty of seafloor characteristics and ecological phenomena were observed through the four deep-towed vehicles. The seafloor survey results, including the video data and the samples of animals, sediments, and mounds, have been provided to different scientific teams for conducting research on marine geophysics, marine geology, marine geochemistry, and marine ecology. The video data can be cross-checked and used as the supporting evidence for the analysis results from the scientific researchers.

The rest of the paper is organized as follows. Section 2 introduces the four deep-towed vehicles developed by the IUT for seafloor imaging and sampling. Section 3 presents the survey results obtained at five important survey sites offshore northeastern Taiwan in 2016 and 2017. Section 4 summarizes the survey results obtained offshore northeastern Taiwan in 2016 and 2017. Section 5 concludes the paper.

2. DEEP-TOWED VEHICLES OF IUT

In the investigation of marine mineral resources, seafloor imaging in combination with samples and seismic data is valuable in the understanding of physical and chemical processes and life taking place in benthic environments. The Woods Hole Oceanographic Institution (WHOI) in collaboration with the DeepSea Power and Light (DSPL) developed the Towed Digital Camera and Multi-rock Coring System (TowCam) in 2003 to facilitate seafloor observation (Fornari 2003). In 2006, the TowCam was introduced to Taiwan through the CGS gas-hydrate program to perform gas hydrate surveys offshore southwestern Taiwan (Lin et al. 2006; Chen et al. 2010). The TowCam built for Taiwan in 2006 is a deep-towed camera system capable of taking digital color photos with high resolution while being towed above the seafloor. However, the photos taken by the TowCam are saved inside the camera and can be retrieved only after the TowCam comes back to the surface. Real-time seafloor imagery is not available with the TowCam.

Observing seafloor images in real-time benefits the efficiency of various seafloor investigations. With the support from the National Energy Program (NEP) of Taiwan

since 2013 (Wang et al. 2015), the IUT has developed four deep-towed vehicles, including the ATIS, V-Corer, TVG, and FITS, as shown in Fig. 2, to carry out real-time seafloor imaging and sampling offshore Taiwan (Chen et al. 2017). In the years of 2016 and 2017, the four deep-towed vehicles have been utilized in multiple cruises for the investigation of mineral resources offshore northeastern Taiwan.

2.1 Abyss Twisted-Pair Imaging System (ATIS)

The ATIS was developed as a deep-towed vehicle for seafloor imaging. As shown in Fig. 2, the ATIS is equipped with a video camera, LED lights, an altimeter with depth sensor, a USBL transponder, and batteries. The working principle of the ATIS is shown in Fig. 3. The ATIS needs to be towed behind a supporting surface vessel through a CTD twisted-pair cable. The viewing system and sensors can be turned on or off via a graphical user interface (GUI), and the required commands are transmitted from the surface vessel to the ATIS through the CTD twisted-pair cable. On the other hand, the sensor data and image data are transmitted from the ATIS to the surface vessel through the CTD twisted-pair cable as well. The acoustic signals for USBL underwater positioning are transmitted between the shipboard transceiver and the subsea transponder directly through the water column. The altitude, depth, and position of the ATIS and the seafloor live video are displayed on the corresponding GUIs. The ATIS is typically towed behind the surface vessel at a speed of roughly 1 knot and is kept about 3 - 5 m above the seafloor. The altitude of the ATIS is adjusted manually by the winch operator based on the real-time sensor data and image data relayed from the ATIS to the surface vessel.

2.2 Video-Guided Multi-Corer (V-Corer)

The V-Corer was developed as a deep-towed vehicle for video-guided seafloor coring. As shown in Fig. 2, the V-Corer is a multi-corer equipped with a video camera, LED lights, an altimeter with depth sensor, a USBL transponder, and batteries. The working principle of the V-Corer is shown in Fig. 4. Such as the ATIS, the V-Corer needs to be towed behind a supporting surface vessel through a CTD twisted-pair cable. The viewing system and sensors can be turned on or off via a GUI, and the required commands are transmitted from the surface vessel to the V-Corer through the CTD twisted-pair cable. Meanwhile, the sensor data and image data are transmitted from the V-Corer to the surface vessel through the CTD twisted-pair cable as well. The acoustic pulses for USBL underwater positioning are transmitted between the shipboard transceiver and the subsea transponder directly through the water column. The altitude, depth, and position of the V-Corer and the seafloor live video are displayed on the corresponding GUIs. Such as the ATIS, the

V-Corer is generally towed behind the surface vessel at a speed of roughly 1 knot and is maintained approximately 3 - 5 m above the seafloor. The altitude of the V-Corer is adjusted manually by the winch operator based on the real-time sensor data and image data relayed from the V-Corer to the surface vessel. Once a sampling area is determined based on the real-time seafloor video, the V-Corer will be lowered to the seafloor to activate the sampling by penetrating the core tubes into the sediment. When the sampling is completed, the V-Corer will be retrieved back to the surface vessel.

2.3 TV-Guided Grabber (TVG)

The TVG was developed as a deep-towed vehicle for

video-guided seafloor sampling. As shown in Fig. 2, the TVG is a grab bucket equipped with three video cameras, LED lights, an altimeter with depth sensor, a USBL transponder, and batteries. The working principle of the TVG is shown in Fig. 5. Such as the ATIS and V-Corer, the TVG needs to be towed behind a supporting surface vessel through a CTD twisted-pair cable. The viewing system and sensors can be turned on or off and the grab bucket can be opened or closed through a GUI. The required commands are transmitted from the surface vessel to the TVG through the CTD twisted-pair cable. On the other hand, the sensor data and image data are transmitted from the TVG to the surface vessel through the CTD twisted-pair cable as well. The acoustic signals for USBL underwater positioning are

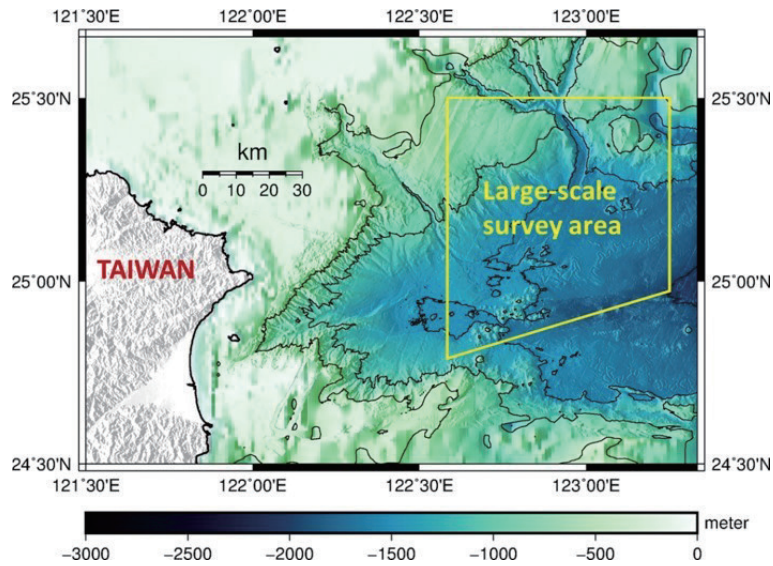


Fig. 1. Large-scale survey area for mineral resource investigation off NE Taiwan in 2016 and 2017.

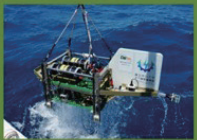

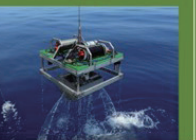

	ATIS	V-Corer	TVG	FITS
Vehicle				
Depth rating	3,000 m			
Viewing system	22,000 lm LED lights Full HD IP camera		22,000 lm LED lights 4K camera x2 SD camera x1	120,000 lm LED lights Full HD IP camera x2 Canon EOS 6D/Canon EF 16-35 mm f/4L IS USM
Tether	8,000 m CTD twisted-pair cable			2,500 m armored electrical/FO cable
Power source	Rechargeable lithium ion batteries, 53 Ah@14.4 VDC			Surface power supply, 5 kW@600 VDC
Sensors	Altimeter, Depth sensor, USBL transponder			Altimeter, Depth sensor, Scanning sonar, Side scan sonar, MBES, INS/DVL, USBL transponder

Fig. 2. Deep-towed vehicles developed by the IUT.

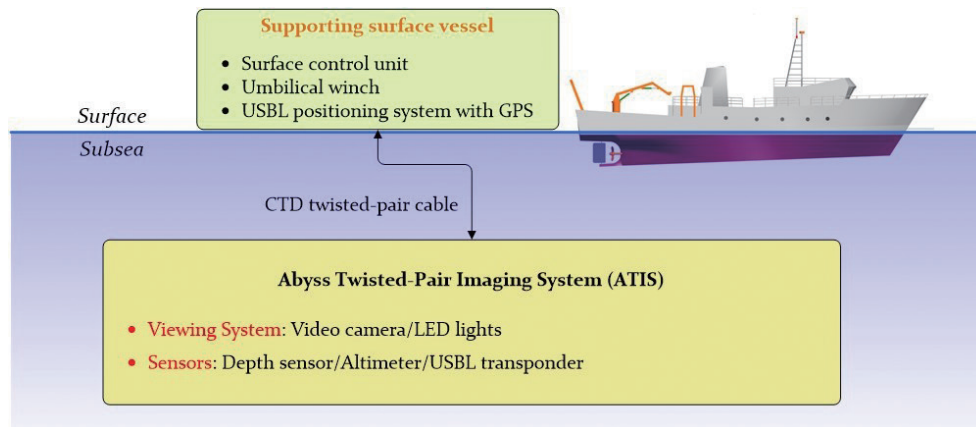


Fig. 3. Working principle of the ATIS.

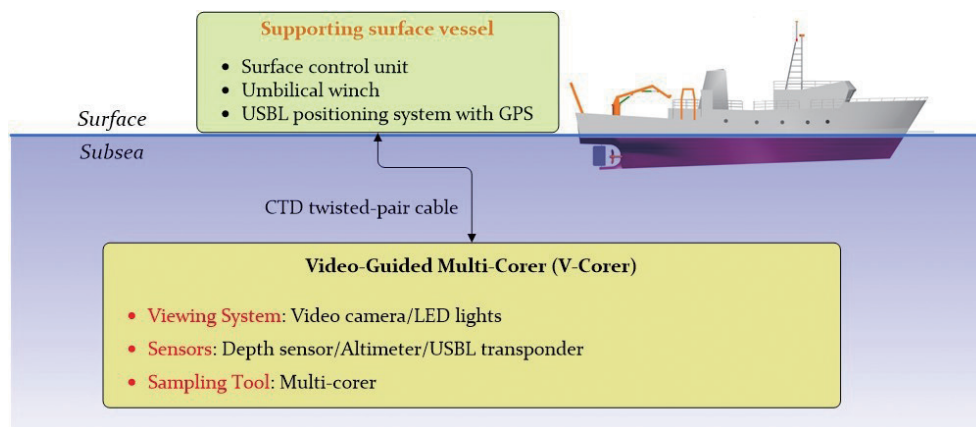


Fig. 4. Working principle of the V-Corer.

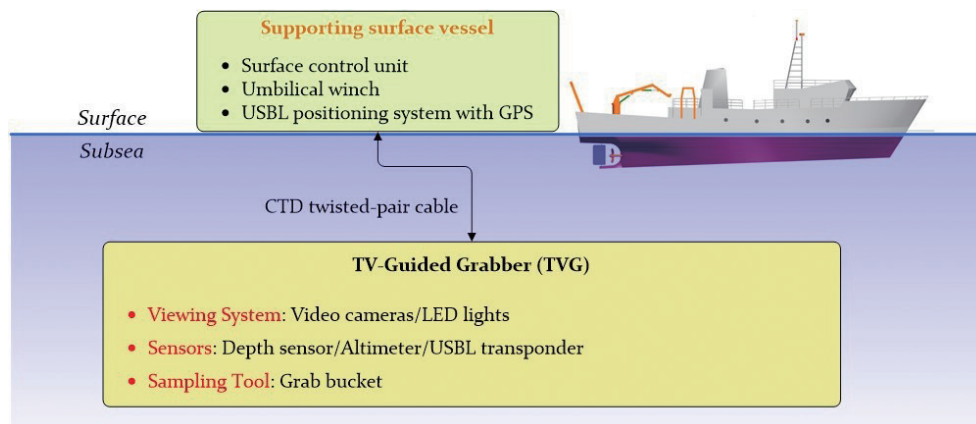


Fig. 5. Working principle of the TVG.

transmitted between the shipboard transceiver and the subsea transponder directly through the water column. The altitude, depth, and position of the TVG and the seafloor live video are displayed on the corresponding GUIs. Such as the ATIS and V-Corer, the TVG is typically towed behind the surface vessel at a speed of roughly 1 knot and is kept about 3 - 5 m above the seafloor. The altitude of the TVG is adjusted manually by the winch operator based on the real-time sensor data and image data relayed from the TVG to the surface vessel. Once a sampling area is determined based on the real-time seafloor video, the TVG will be lowered to the seafloor and the grab bucket will be closed to catch and secure the samples. When the sampling is completed, the TVG will be retrieved back to the surface vessel.

2.4 Fiber-Optical Instrumentation Towed System (FITS)

The FITS was developed as a deep-towed vehicle for seafloor imaging and sensing. As shown in Fig. 2, the FITS is equipped with two video cameras, a still image camera, LED lights, an altimeter with depth sensor, a USBL transponder, an inertial navigation system (INS), a Doppler velocity log (DVL), a scanning sonar, a side scan sonar, and a multi-beam echo sounder (MBES). The working principle of the FITS is shown in Fig. 6. The FITS needs to be towed behind a supporting surface vessel through an armored electrical/fiber-optic cable. The viewing system and sensors can be turned on or off via a GUI, and the required commands are transmitted from the surface vessel to the FITS through the electrical/fiber-optic cable. On the other hand, the sensor data and image data are transmitted from the FITS to the surface vessel through the electrical/fiber-optic cable as well. The acoustic pulses for USBL underwater positioning are transmitted between the shipboard transceiver and the subsea transponder directly through the water column. The altitude, depth, and position of the FITS, the sonar images,

and the seafloor live video are displayed on the corresponding GUIs. For seafloor optical imaging, the FITS is typically towed behind the surface vessel at a speed of roughly 1 knot and is kept about 5 - 7 m above the seafloor. For seafloor mapping with the MBES, the FITS is generally towed behind the surface vessel at a speed of between 2 to 4 knots and is maintained between 20 - 30 m above the seafloor. The altitude of the FITS is adjusted manually by the winch operator based on the real-time sensor data and image data relayed from the FITS to the surface vessel.

2.5 Comparisons Among IUT Deep-Towed Vehicles

Real-time visual seafloor observation is one of the main characteristics of the ATIS. High portability is another critical concern in the design of the ATIS. The ATIS transmits live video stream and sensor data through a twisted-pair or coaxial cable up to 8000 m. The communication over an 8000-m long twisted-pair or coaxial cable provides a broadband transmission speed up to 3 Mbps, which enables the ATIS to deliver real-time high-definition (HD) seafloor video at resolution 1920×1080 pixels and frame rate 30 fps. The ATIS is battery-powered, featuring a built-in 14.4 VDC power supply with rechargeable lithium-ion batteries that lasts up to 4 - 5 h when fully charged.

For the sake of surface geochemical analysis, a multi-corer is typically utilized to collect undisturbed sediments from the seafloor. If the seafloor condition at a coring site is unclear or unavailable, a conventional multi-corer will be very likely to encounter the following situations: (1) it fails to reach the bottom; (2) it fails to get close to the desired location; (3) it fails to collect samples; and (4) it is damaged by striking the hard bottom. As opposed to conventional blind corers, the V-Corer was developed to provide real-time visual information of the coring sites to the scientists such that a prompt and accurate decision can be made for collecting coring samples during surveys. As shown in Fig. 2, the V-Corer

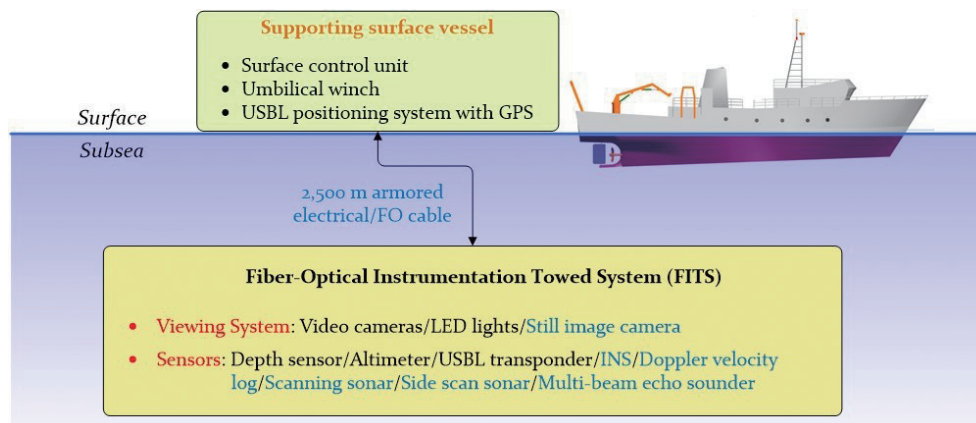


Fig. 6. Working principle of the FITS.

was developed by integrating the viewing system, power source, and sensors of the ATIS with a multi-corer. Thus, the V-Corer is able to uplink HD live video streams and sensor data to the surface vessel, which significantly improves the efficiency and safety of sediment sampling operation. Additionally, the context images of the coring sites provide important clues and information for the collected samples.

The TVG was designed to collect rocks, hard/soft sediments, and marine creatures from the seafloor. It has the same power and communication architectures as the ATIS and V-Corer. As shown in Fig. 2, the TVG is equipped with three high resolution cameras for observing the seafloor and monitoring the grab bucket from different view angles. An underwater actuator installed on the TVG provides the mechanical energy to open and close the grab bucket. Such as the ATIS and V-Corer, the TVG can transmit HD live video streams and sensor data back to the surface vessel to provide researchers with real-time information for making proper decisions on where to grab samples during surveys.

The ATIS is battery-powered and its 4 - 5 h of endurance imposes the operator to launch and recover the ATIS often and costly for completing a seafloor survey. Thus, in 2014, the FITS was designed and built to obtain the surface power by a hybrid electric/fiber-optic umbilical, so that it has nearly unlimited endurance and supports a bandwidth of gigabits per second. With unlimited power supply and high bandwidth budget, the FITS can carry more sensors and instruments than the ATIS to collect seafloor data. As shown in Fig. 2, in addition to video cameras and LED lights, a scanning sonar, a side scan sonar, and an MBES are mounted on the FITS to enable wide range seafloor survey for seabed feature mapping. Moreover, an INS and a DVL are also mounted on the FITS for precise underwater positioning.

In order to obtain videos with better quality, six 300-watt LED lights constitute the lighting system of the FITS, which produces 120000 lumens to increase illuminance of the seafloor. Meanwhile, increasing the lumen output also allows the FITS to be towed at a higher altitude above the seafloor for survey purposes, which reduces the risk of collision on the seafloor. Although the video cameras on the ATIS and the FITS provide HD-quality images, the image resolution of 1920×1080 pixels (about 2 megapixels) is still not high enough for identifying detailed seafloor features. Therefore, a still camera is installed on the FITS to capture photos with resolution of 5472×3648 pixels (about 20 megapixels) to provide high resolution images for objects of interest.

2.6 Scientific Impact of IUT Deep-Towed Vehicles

In recent years, since issues regarding climate change, energy demand, and environmental protection become more significant than before, marine scientific research gets close attention globally and nationally. In Taiwan, the instruments

and devices required for marine scientific research are mostly commercial products purchased from foreign companies; there is relatively little manpower and few resources devoted to the development of marine engineering technologies. With standard instruments and devices, the thinking and experimental methods of domestic scientific teams are probably close to those of foreign scientific teams. It is difficult to create unique research topics in Taiwan under this circumstance. Domestic scientists might be deterred by the high prices or other factors of the instruments and devices customized to conduct unique experiments. On the other hand, because the instruments and devices are purchased from foreign companies, it is difficult for domestic scientists to break free from limitations in order to possess full dominance on scientific issues.

The IUT deep-towed vehicles have enabled many marine scientists in Taiwan to free themselves from the amounts of time required to wait for the equipment rented or introduced from overseas to arrive in Taiwan. As a result, the IUT deep-towed vehicles have enabled many marine scientists in Taiwan to schedule the experiments more effectively for their marine ecological, marine chemical, and marine geological research. By means of the IUT deep-towed vehicles, which can be operated via three small and medium-sized national research vessels in Taiwan including Ocean Researcher I (OR1), Ocean Researcher II (OR2), and Ocean Researcher III (OR3), many marine scientists in Taiwan have obtained scientific data and samples from the seafloor offshore southwestern and northeastern Taiwan, which could not be acquired before by divers or traditional sampling methods. The information and details extracted from those scientific data and samples facilitate domestic marine scientists in solving scientific puzzles. The IUT deep-towed vehicles are also constantly utilized in government sponsored seafloor survey projects and keep contributing to deep-sea investigation and exploration in Taiwan.

3. SEAFLOOR SURVEYS OFF NE TAIWAN

For the 4-year CGS program, "Geological Investigation of Mineral Resource Potential in the Offshore Northeastern Taiwan", the large-scale survey area for 2016 and 2017 is located at the southern Okinawa Trough from $E122^{\circ}35'$ to $E123^{\circ}15'$ and from $N24^{\circ}47.32'$ to $N25^{\circ}30'$, as shown in Fig. 1. According to the high-resolution topographic data, site Mienhua Volcano (MHV) has a wide range of cones and has clear relief features around the seafloor (Hsu 2017). Gas plumes are observed at sites Penglai Fault Zone (PFZ), Geolin Mounds (GLM), and Fire Dragon Volcano 1 (FDV-1); based on the inversion results from the deep-towed magnetic data, most of the gas flares out of the seabed are roughly located in relatively low susceptibility areas such as sites PFZ and GLM (Hsu 2017). In addition, at site Yonaguni Knoll IV-1 (YK4-1), geochemical and geothermal

investigations show considerable features relating to hydrothermal mineral fields while no significant features are observed on seismic data (Liu 2017). Investigation results of sites GLM and PFZ reveal high potential for hydrothermal activities at both sites. Site MHV is located at the south of the Mian-Hua Canyon where geophysical data indicate that there should be some hydrothermal activities or related features (Liu 2017). Based on the above large-scale survey results, YK4-1, PFZ, MHV, FDV-1, and GLM are chosen as the survey sites for seafloor video surveys and sampling, as shown in Fig. 7.

3.1 Site Yonaguni Knoll IV-1 (YK4-1)

A total of 10 survey tracks covering 26.21 km are completed at site YK4-1 through cruises OR1-1139, OR3-

1942, and OR1-1164, as shown in Fig. 8. In addition to flat soft sediments, many mounds are also observed at site YK4-1, as shown in Fig. 9. Several hydrothermal activities are found in the vicinity of the location (N24°50'57.00", E122°42'02.40"). In addition, hydrothermal plumes and lots of squat lobsters (*Shinkaia crosnieri*) are observed at the location (N24°50'49.92", E122°42'02.58"), as shown in Fig. 9.

Three sampling operations are successfully conducted using the TVG at site YK4-1, as shown Fig. 10. At location A1-L-TVG, squat lobsters and mussels are observed to be distributed on some mounds, and a small amount of mussels and squat lobsters are collected by the TVG, as shown in Fig. 10. On the other hand, at location A1-M-TVG1, lots of sediments are collected by the TVG, as shown in Fig. 10. Along each survey track, the distributed length of mounds

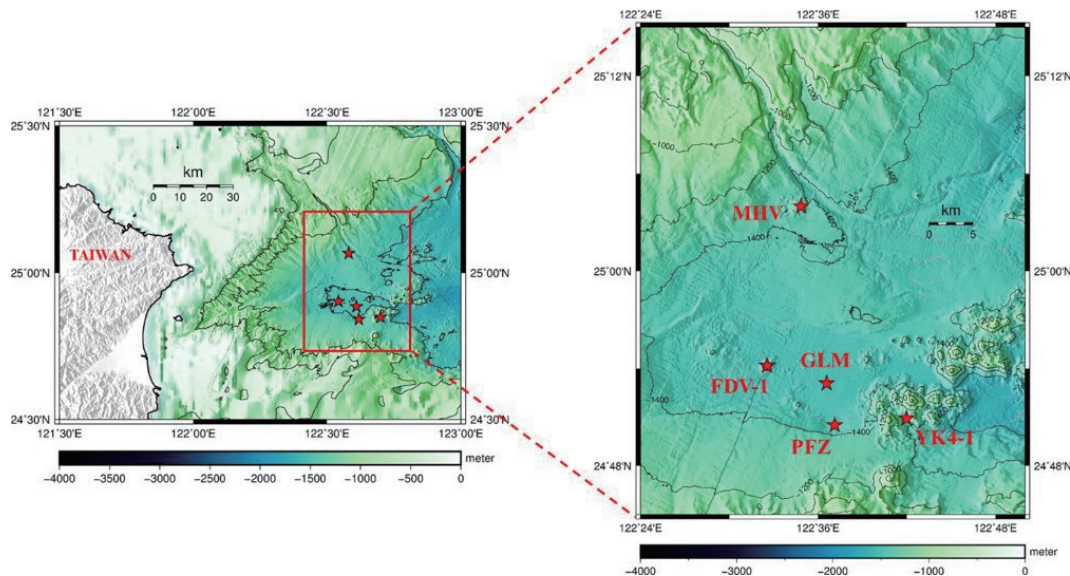


Fig. 7. Survey sites for seafloor video surveys and sampling off NE Taiwan in 2016 and 2017.

Survey track	Length of survey track (km)	Distributed length of mounds (km)
SV1-1139-VCorer-Dive04-1-SG	1.07	0.01
SV1-1139-VCorer-Dive07-1-SG	1.01	0.52
SV1-1139-VCorer-Dive08-1-SG	1.32	0.86
SV3-1942-ATIS-Dive02-1-SG	2.27	0.16
SV3-1942-ATIS-Dive06-1-SG	6.45	0.06
SV3-1942-ATIS-Dive07-1-SG	8.89	0.13
SV3-1942-ATIS-Dive08-1-SG	2.24	0.77
SV1-1164-TVG-Dive02-1-UU	2.33	1.35
SV1-1164-TVG-Dive03-1-SG	0.29	0.04
SV1-1164-TVG-Dive04-1-UU	0.34	0.07
Total	26.21	3.97

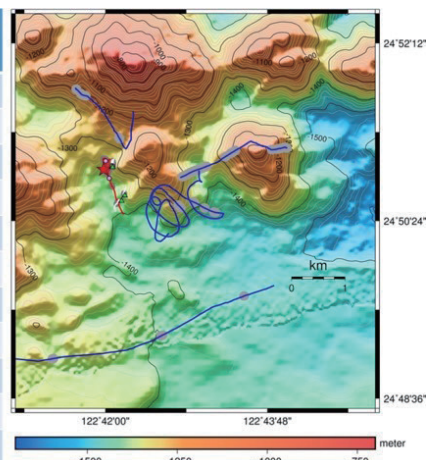


Fig. 8. Survey tracks at site YK4-1.

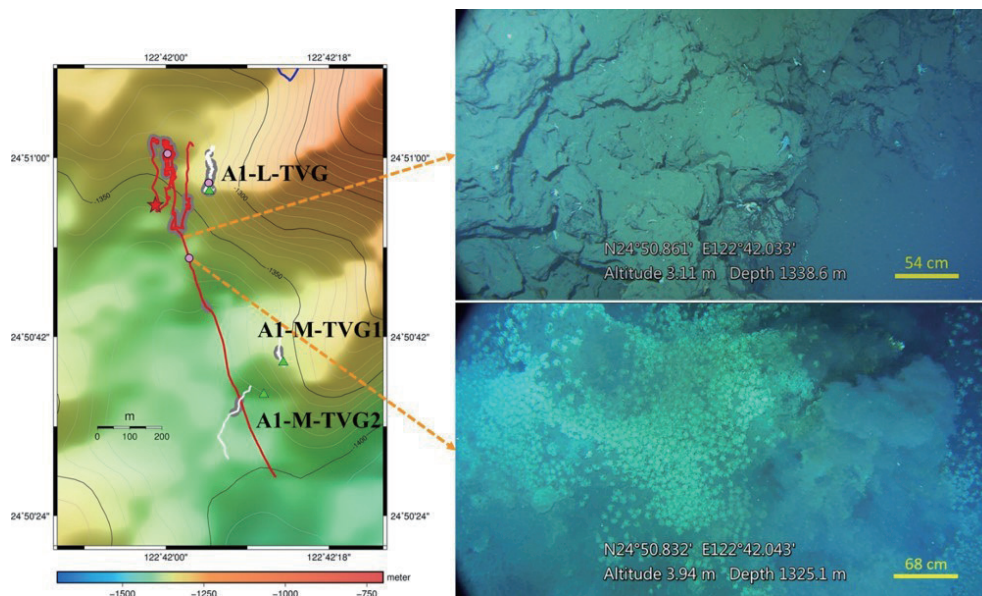


Fig. 9. Mounds, hydrothermal plumes, and squat lobsters are observed at site YK4-1.

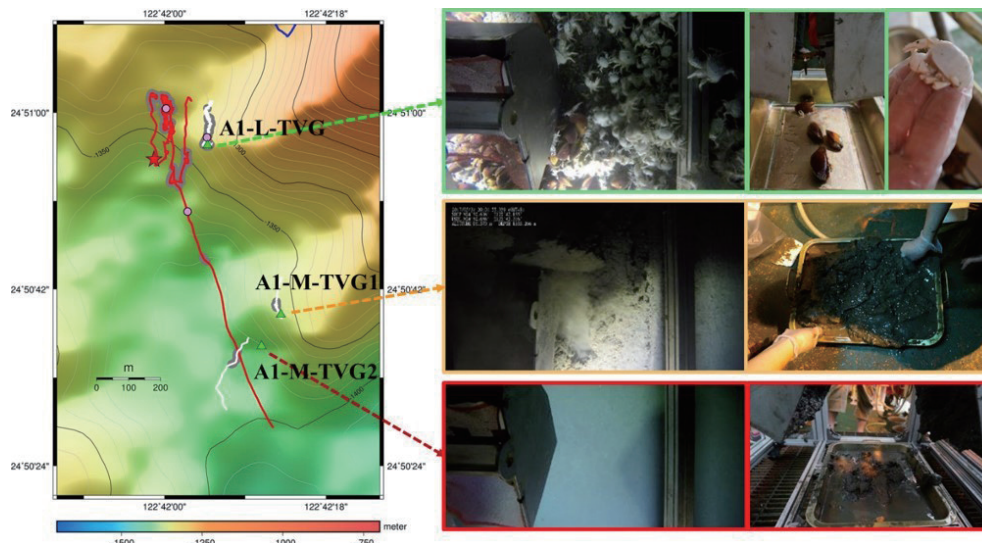


Fig. 10. Mussels, squat lobsters, and sediments are collected at site YK4-1.

is estimated and listed in Fig. 8 as well. The total distributed length of mounds along the 10 survey tracks is estimated to be 3.97 km.

3.2 Site Penglai Fault Zone (PFZ)

A total of nine survey tracks covering 27.09 km are completed at site PFZ through cruises OR1-1139, OR3-1942, OR1-1164, OR3-2012A, and OR3-2012B, as shown in Fig. 11. Mounds are found to be distributed within a radius of roughly 500 m from the location (N24°50'58.86",

E122°37'15.42"), shown in Fig. 12. Through the locations in which mounds are found, the distributed area of mounds at site PFZ, the shaded area in Fig. 12, is estimated to be 0.21 km². Near the location (N24°50'58.86", E122°37'15.42"), the seawater temperature is detected to increase from 4.6°C to 4.8°C ~ 5.1°C, as shown in Fig. 13. Meanwhile, mounds with several meters of height and mussels distributed on the mounds are also observed near the above location. Moreover, the TVG collides with the mound several times at the above location, such that the TVG brings back several small mound samples, which are found to have

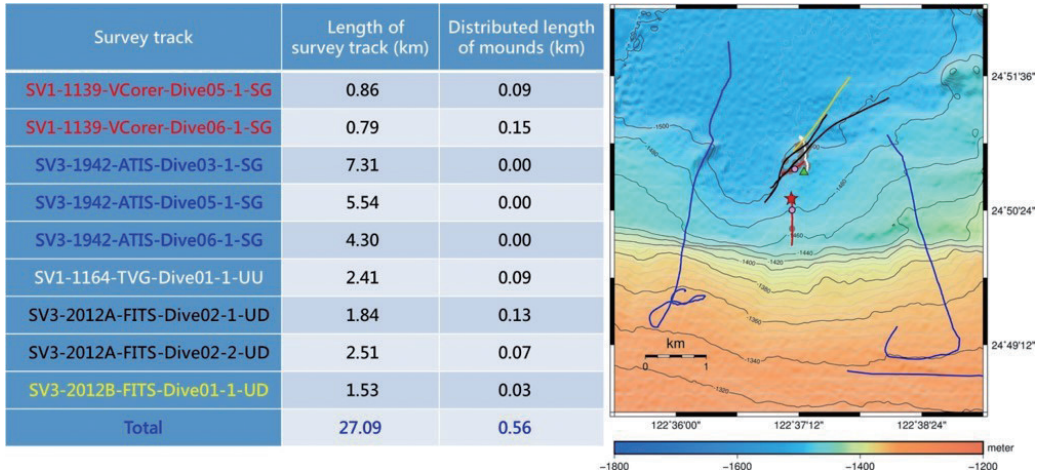


Fig. 11. Survey tracks at site PFZ.

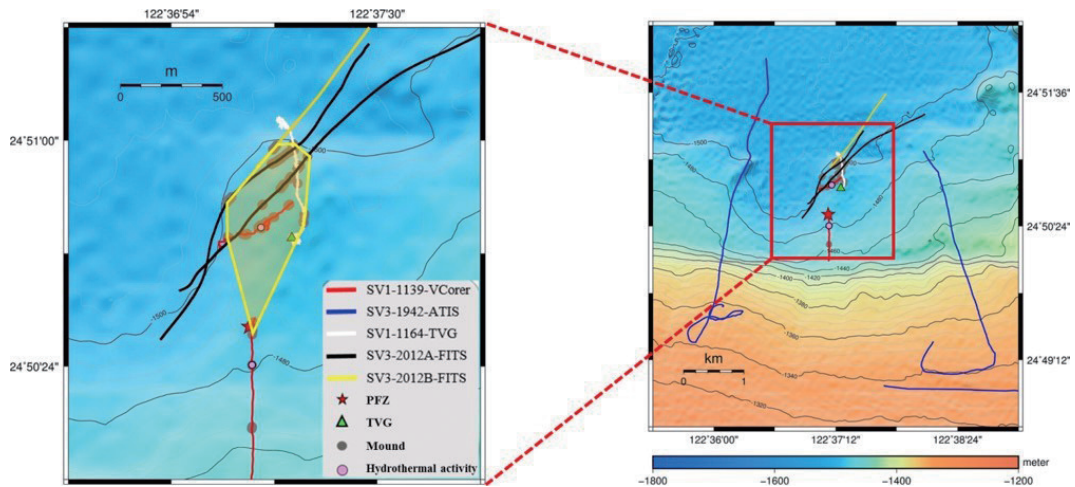


Fig. 12. Estimated area of mounds at site PFZ.

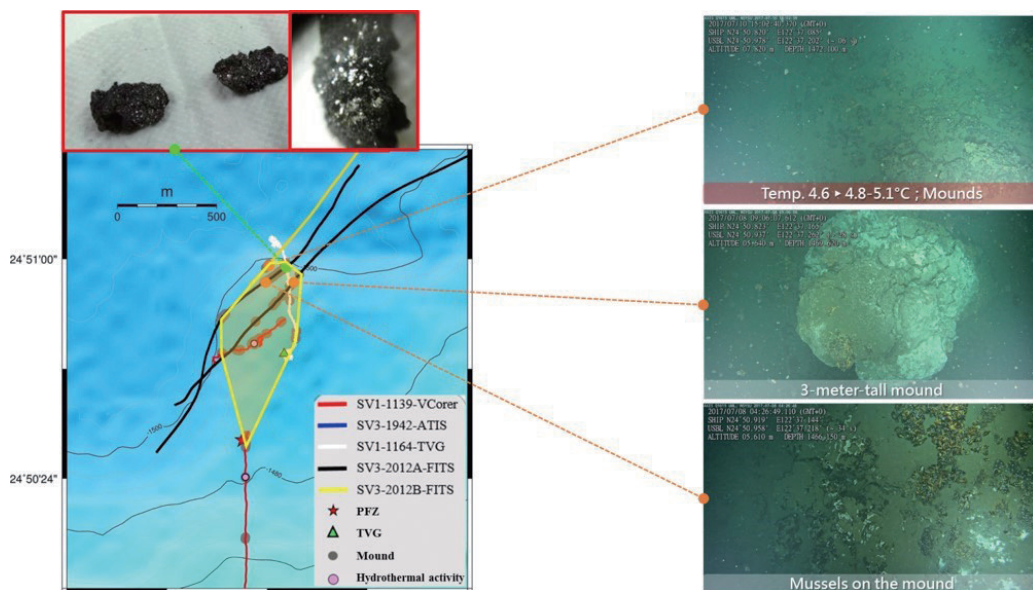


Fig. 13. Seafloor images and mound samples obtained in estimated area of mounds at site PFZ.

metallic or crystal reflections, as shown in Fig. 13. In addition, hydrothermal fissures are observed near the location marked as a star (PFZ) in Fig. 13. Along each survey track, the distributed length of mounds is estimated and listed in Fig. 11 as well. The total distributed length of mounds along the nine survey tracks is estimated to be 0.56 km.

3.3 Site Mienhua Volcano (MHV)

A total of four survey tracks covering 8.87 km are

completed at site MHV through cruises OR3-2012A and OR3-2012B, as shown in Fig. 14. The center of site MHV is a volcano. Mussels, squat lobsters, gas seeps, and empty mussel shells are found on the mounds located in the flat area on the east side of the volcano, as shown in Fig. 15. The seawater temperature is detected to increase from 4.4°C ~ 4.5°C - 4.6°C at the location (N25°03'38.94", E122°35'34.20"), as shown in Fig. 15. The increase of the seawater temperature is also observed at another location. Mounds with several meters of height are found in the uplift

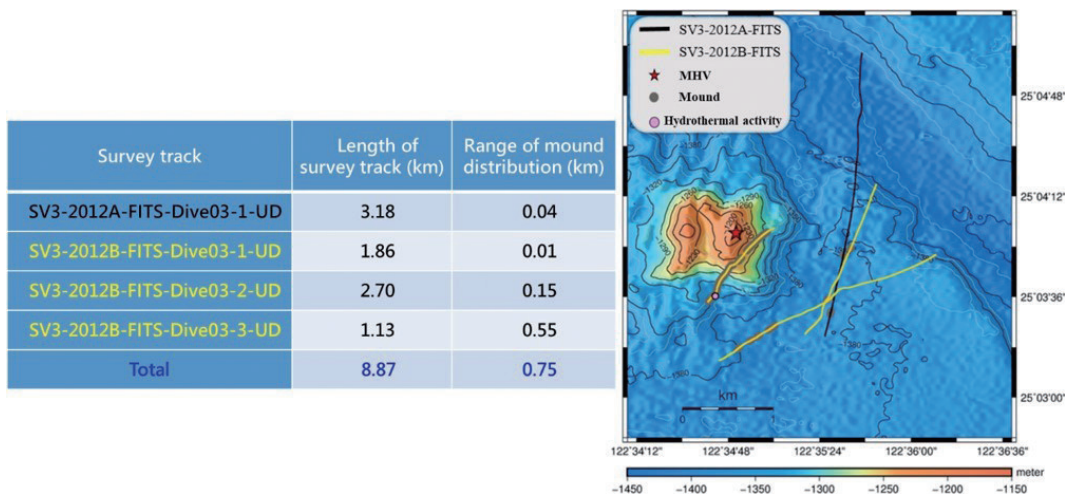


Fig. 14. Survey tracks at site MHV.

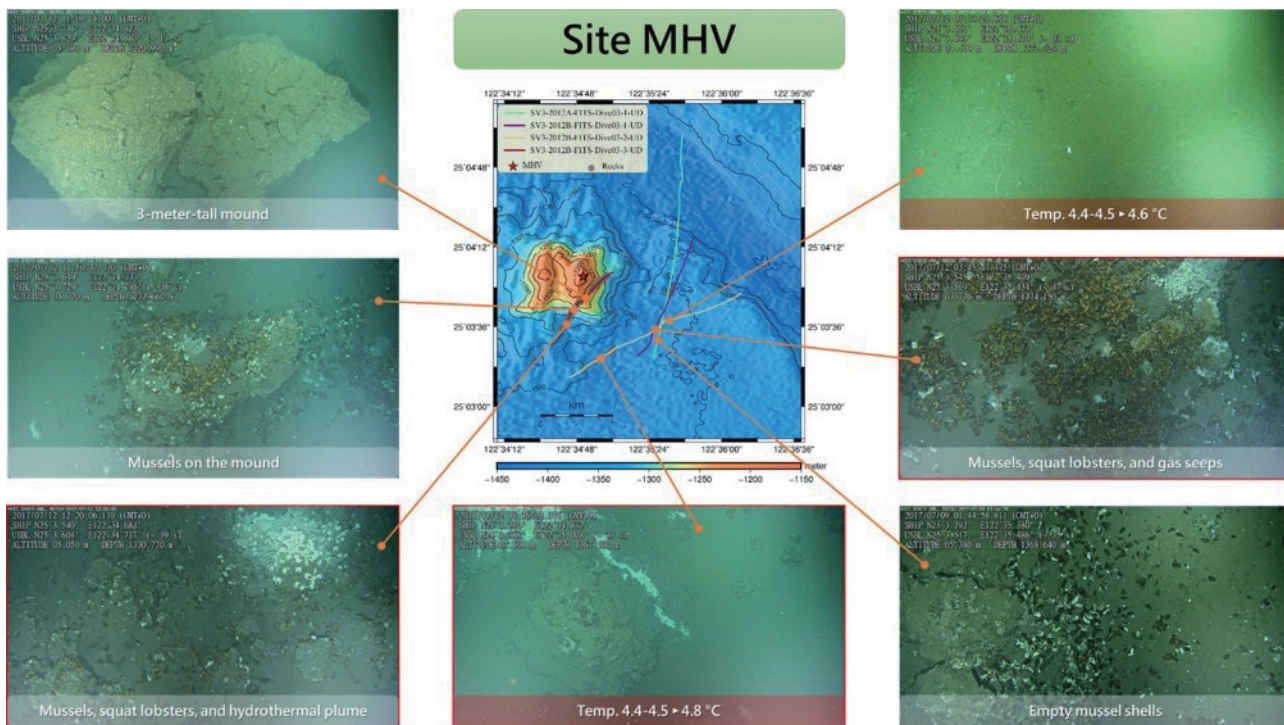


Fig. 15. Seafloor images obtained at site MHV.

area of the volcano, but no biotic communities are observed on the mounds. Mussels, squat lobsters, and hydrothermal activities gradually appear on the mounds in the foothill area on the south side of the volcano, as shown in Fig. 15. A hydrothermal plume is observed on the mound surrounded by a biotic community at the location (N25°03'36.24", E122°34'43.20"). Along each survey track, the distributed length of mounds is estimated and listed in Fig. 14 as well. The total distributed length of mounds along the nine survey tracks is estimated to be 0.75 km.

3.4 Site Fire Dragon Volcano 1 (FDV-1)

For site FDV-1, only two survey tracks covering 4.22 km are completed in 2017 through cruise OR3-2012B, as shown in Fig. 16. Mounds are found to be widely distributed along the two survey tracks at site FDV-1, as shown in Fig. 17. Empty mussel shells on the mound, corals on the mound, huge mounds, and mounds with several meters of height are observed along the survey tracks. Meanwhile, no observations related to the seawater temperature increase and

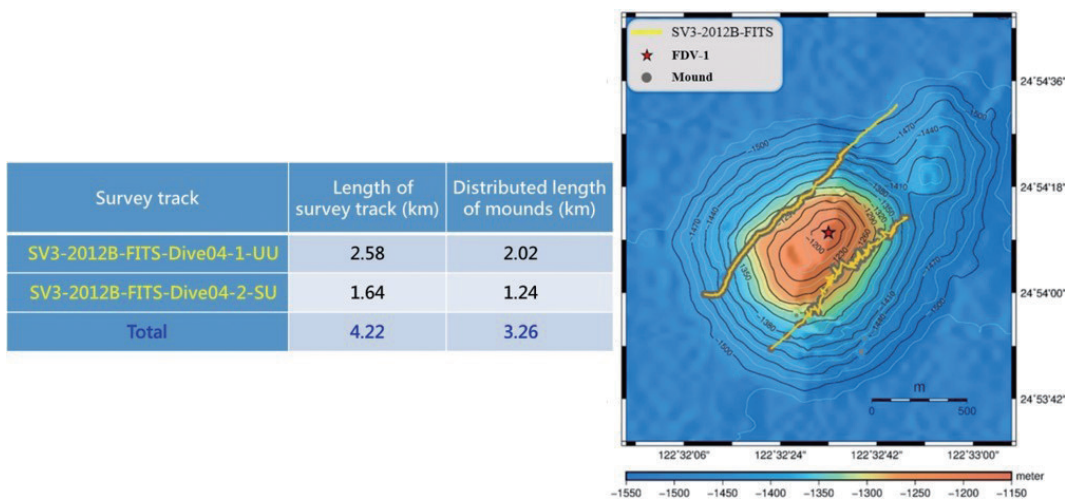


Fig. 16. Survey tracks at site FDV-1.

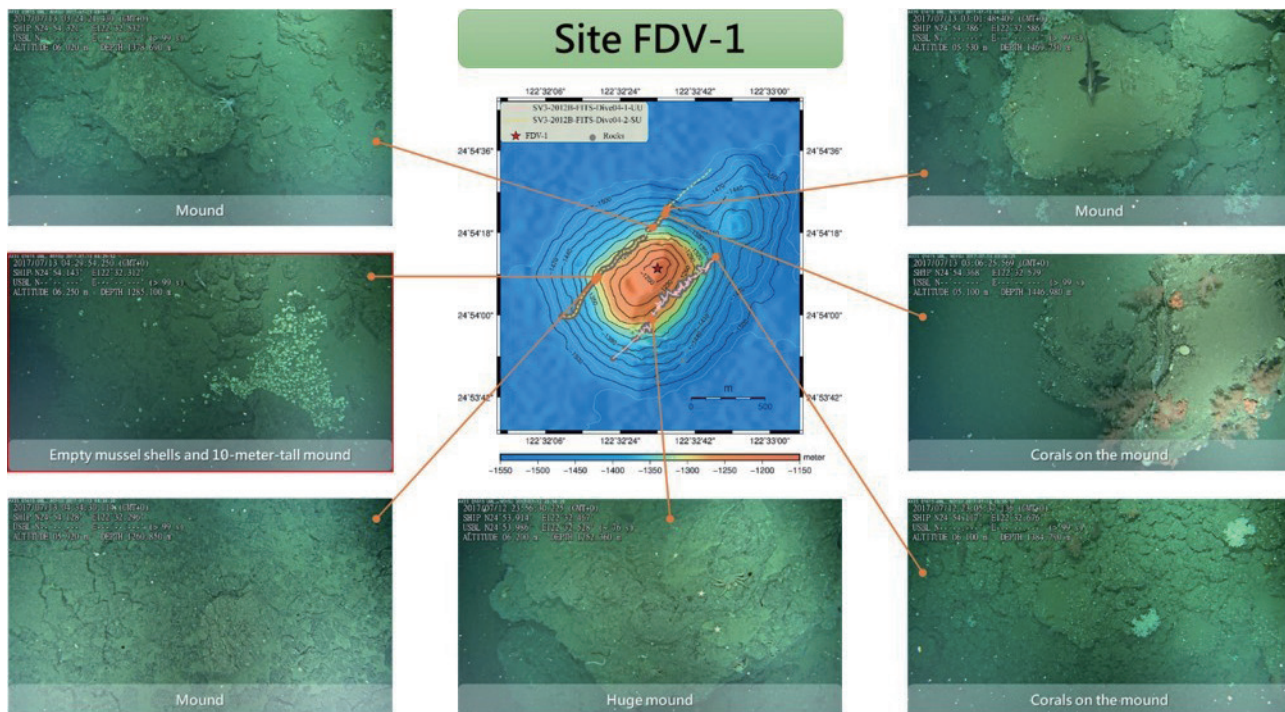


Fig. 17. Seafloor images obtained at site FDV-1.

the hydrothermal activity are obtained. Along each survey track, the distributed length of mounds is estimated and listed in Fig. 16 as well. The total distributed length of mounds along the nine survey tracks is estimated to be 3.26 km.

3.5 Site Geolin Mounds (GLM)

A total of six survey tracks covering 16.3 km are completed at site GLM through cruises OR3-2012A and OR3-2012B, as shown in Fig. 18. A large amount of mounds are observed within a radius of 500 m from the center of site GLM (N24°53.15', E122°36.58'), as shown in Fig. 19. Through the locations in which mounds are found, the distributed area of mounds at site GLM, the shaded area in Fig. 19, is estimated to be 0.27 km². Some of the mounds are found to have clusters of squat lobsters and mussels on top of them, as shown in Fig. 20. The seawater temperature is detected to increase from 4.5°C to 6.8°C ~ 7.6°C near the center of site GLM. In addition, five active hydrothermal chimneys are observed at site GLM, and one of them is shown in Fig. 20, where the seawater temperature is detected to increase from 4.5 - 5.4°C. Moreover, along each survey track, the distributed length of mounds is estimated and listed in Fig. 18 as well. The total distributed length of mounds along the six survey tracks is estimated to be 0.93 km.

4. SURVEY RESULTS SUMMARY

The seafloor features observed at sites YK4-1, PFZ, MHV, FDV-1, and GLM are listed in Table 1. Phenomena of smoke, bubbles, and fluids were observed at four survey sites including YK4-1, PFZ, MHV, and GLM. Increase of the seawater temperature was detected at three survey sites including PFZ, MHV, and GLM. Mounds were observed at five survey sites including YK4-1, PFZ, MHV, FDV-1, and GLM. The phenomenon of white substance covering on the mounds or seafloor was observed at three survey sites including PFZ, MHV, and GLM. Biological communities were observed at four survey sites including YK4-1, PFZ, MHV, and GLM. Empty mussel shells were observed at two survey sites including MHV and FDV-1.

The types and coordinates of hydrothermal activities observed at four survey sites including YK4-1, PFZ, MHV, and GLM are listed in Table 2. The latitude and longitude of the surface research vessel (R/V) are utilized to denote the locations where underwater positioning data are not obtained.

The smoke phenomenon was found at sites YK4-1 and GLM, as shown in Table 2. At site YK4-1, the smoke phenomenon was found through the V-Corer at one location, (N24°50.832', E122°42.043'), on survey track SV1-1139-VCorer-Dive04-1 during cruise OR1-1139; the location of the observed smoke phenomenon is denoted using the coordinates of the surface R/V Ocean Researcher I. At site GLM, the smoke phenomenon was found through the FITS

at five locations, including (N24°53.164', E122°36.598'), (N24°53.148', E122°36.583'), (N24°53.137', E122°36.572'), (N24°53.131', E122°36.566'), and (N24°53.006', E122°36.426'), on survey track SV3-2012B-FITS-Dive02-2 during cruise OR3-2012B; the locations of the observed smoke phenomenon are denoted using the coordinates of the subsea FITS.

The fluid phenomenon was found at sites YK4-1, PFZ, MHV, and GLM, as shown in Table 2. At site YK4-1, the fluid phenomenon was found through the V-Corer at one location, (N24°51.007', E122°42.003'), on survey track SV1-1139-VCorer-Dive08-1 during cruise OR1-1139; the location of the observed fluid phenomenon is denoted using the coordinates of the surface R/V Ocean Researcher I. At site PFZ, the fluid phenomenon was found through the V-Corer at two locations, including (N24°50.404', E122°37.135') and (N24°50.769', E122°37.161'), on survey tracks, SV1-1139-VCorer-Dive05-1 and SV1-1139-VCorer-Dive06-1, respectively, during cruise OR1-1139; the location of the observed fluid phenomenon is denoted using the coordinates of the surface R/V Ocean Researcher I. At site MHV, the fluid phenomenon was found through the FITS at one location, (N25°03.604', E122°34.717'), on survey track SV3-2012B-FITS-Dive03-3 during cruise OR3-2012B; the location of the observed fluid phenomenon is denoted using the coordinates of the subsea FITS. At site GLM, the fluid phenomenon was found through the FITS at one location, (N24°53.553', E122°37.088'), on survey track SV3-2012A-FITS-Dive01-3 during cruise OR3-2012A; the location of the observed fluid phenomenon is denoted using the coordinates of the subsea FITS.

The bubble phenomenon was found at site YK4-1, as shown in Table 2. At site YK4-1, the bubble phenomenon was found through the TVG at one location, (N24°50.958', E122°42.079'), on survey track SV1-1164-TVG-Dive02-1 during cruise OR1-1164; the location of the observed bubble phenomenon is denoted using the coordinates of the subsea TVG.

The coordinates of biological communities observed at four survey sites including YK4-1, PFZ, MHV, and GLM are listed in Table 3.

At site YK4-1, biological communities were found in three survey cruises, as shown in Table 3. During cruise OR1-1139, biological communities were found through the V-Corer at three locations, including (N24°50.832', E122°42.043'), (N24°50.950', E122°42.005'), and (N24°50.975', E122°42.005'), on survey tracks SV1-1139-VCorer-Dive04-1, SV1-1139-VCorer-Dive07-1, and SV1-1139-VCorer-Dive08-1, respectively; the locations of the observed biological communities are denoted using the coordinates of the subsea V-Corer. In cruise OR3-1942, a biological community was found through the ATIS at one location, (N24°50.940', E122°43.089'), on survey track SV3-1942-ATIS-Dive08-1; the location of the observed

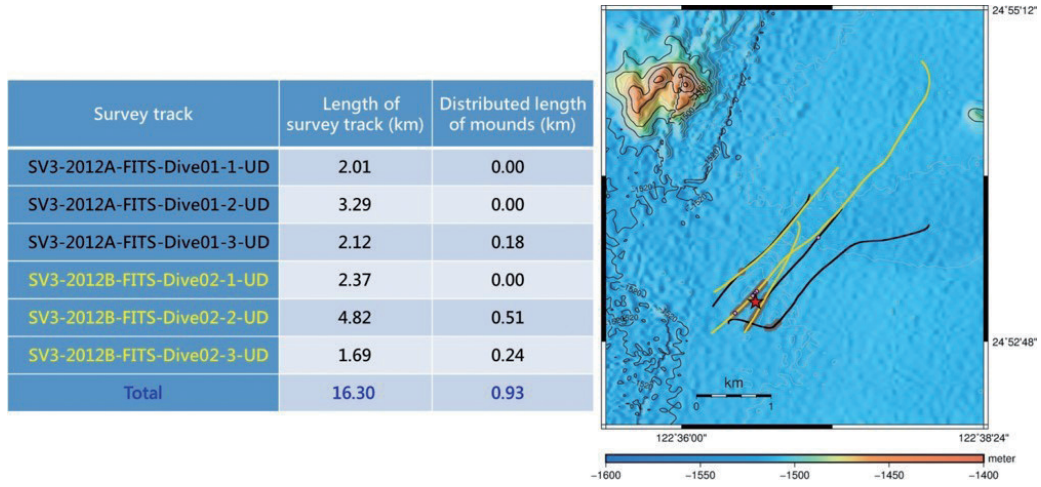


Fig. 18. Survey tracks at site GLM.

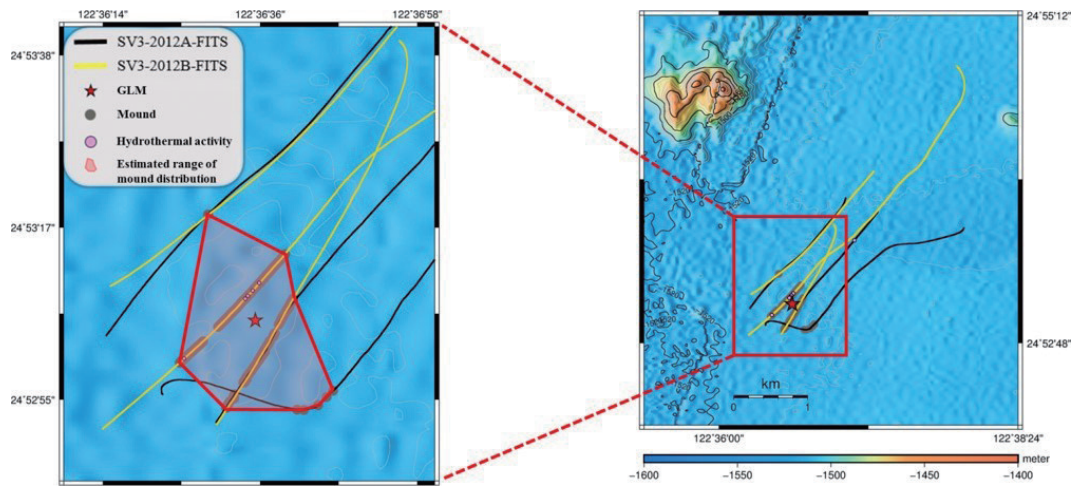


Fig. 19. Estimated area of mounds at site GLM.

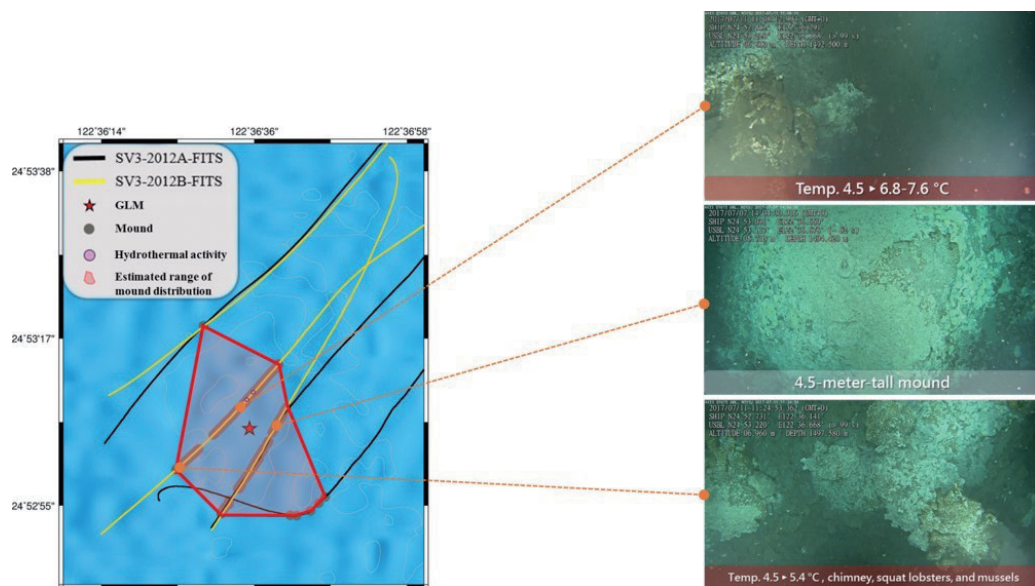


Fig. 20. Seafloor images obtained in the estimated area of mounds at site GLM.

Table 1. Seafloor features at sites YK4-1, PFZ, MHV, FDV-1, and GLM.

Seafloor feature	Survey site				
	YK4-1	PFZ	MHV	FDV-1	GLM
Smoke/Fluids/Bubbles	√	√	√		√
Increase of the seawater temperature		√	√		√
Mounds	√	√	√	√	√
White substance covering on the mounds or seafloor		√	√		√
Biological communities	√	√	√		√
Empty mussel shells			√	√	

Table 2. Types and coordinates of hydrothermal activities observed at sites YK4-1, PFZ, MHV, and GLM.

Survey site	Hydrothermal activity observed	Survey track	Coordinates
YK4-1	Smoke	SV1-1139-VCorer-Dive04-1	* N24°50.832', E122°42.043'
	Fluids	SV1-1139-VCorer-Dive08-1	* N24°51.007', E122°42.003'
	Bubbles	SV1-1164-TVG-Dive02-1	N24°50.958', E122°42.079'
PFZ	Fluids	SV1-1139-VCorer-Dive05-1	* N24°50.404', E122°37.135'
	Fluids	SV1-1139-VCorer-Dive06-1	* N24°50.769', E122°37.161'
MHV	Fluids	SV3-2012B-FITS-Dive03-3	N25°03.604', E122°34.717'
GLM	Smoke	SV3-2012B-FITS-Dive02-2	N24°53.164', E122°36.598'
	Smoke	SV3-2012B-FITS-Dive02-2	N24°53.148', E122°36.583'
	Smoke	SV3-2012B-FITS-Dive02-2	N24°53.137', E122°36.572'
	Smoke	SV3-2012B-FITS-Dive02-2	N24°53.131', E122°36.566'
	Smoke	SV3-2012B-FITS-Dive02-2	N24°53.006', E122°36.426'
	Fluids	SV3-2012A-FITS-Dive01-3	N24°53.553', E122°37.088'

Table 3. Coordinates of biological communities observed at sites YK4-1, PFZ, MHV, and GLM.

Survey site	Survey track	Coordinates
YK4-1	SV1-1139-VCorer-Dive04-1	N24°50.832', E122°42.043'
	SV1-1139-VCorer-Dive07-1	N24°50.950', E122°42.005'
	SV1-1139-VCorer-Dive08-1	N24°50.975', E122°42.005'
	SV3-1942-ATIS-Dive08-1	N24°50.940', E122°43.089'
	SV1-1164-TVG-Dive02-1	N24°50.955', E122°42.077'
PFZ	SV3-2012A-FITS-Dive02-1	N24°50.958', E122°37.218'
MHV	SV3-2012A-FITS-Dive03-1	N25°03.517', E122°35.486'
	SV3-2012B-FITS-Dive03-1	N25°03.569', E122°35.434'
	SV3-2012B-FITS-Dive03-3	N25°03.604', E122°34.717'
	SV3-2012B-FITS-Dive03-3	N25°03.729', E122°34.786'
GLM	SV3-2012B-FITS-Dive02-2	N24°53.220', E122°36.668'

biological community is denoted using the coordinates of the subsea ATIS. In cruise OR1-1164, a biological community was found through the TVG at one location, (N24°50.955', E122°42.077'), on survey track SV1-1164-TVG-Dive02-1; the location of the observed biological community is denoted using the coordinates of the subsea TVG.

At site PFZ, a biological community was found through the FITS at one location, (N24°50.958', E122°37.218'), on survey track SV3-2012A-FITS-Dive02-1 during cruise OR3-2012A, as shown in Table 3; the location of the observed biological community is denoted using the coordinates of the subsea FITS.

At site MHV, biological communities were found in two survey cruises, as shown in Table 3. During cruise OR3-2012A, a biological community was found through the FITS at one location, (N25°03.517', E122°35.486'), on survey track SV3-2012A-FITS-Dive03-1; the location of the observed biological community is denoted using the coordinates of the subsea FITS. During cruise OR3-2012B, biological communities were found through the FITS at three locations, including (N25°03.569', E122°35.434') on survey track SV3-2012B-FITS-Dive03-1 and (N25°03.604', E122°34.717') and (N25°03.604', E122°34.717') on survey track SV3-2012B-FITS-Dive03-3; the location of the observed biological community is denoted using the coordinates of the subsea FITS.

At site GLM, a biological community was found through the FITS at one location, (N24°53.220', E122°36.668'), on survey track SV3-2012B-FITS-Dive02-2 during cruise OR3-2012B, as shown in Table 3; the location of the observed biological community is denoted using the coordinates of the subsea FITS.

The distributed ratio of mounds on each survey track at site YK4-1 is listed in Table 4. A total of ten survey tracks were executed at site YK4-1; the V-Corer was used to execute three survey tracks during cruise OR1-1139; the ATIS was used to execute four survey tracks during cruise OR3-1942; the TVG was used to execute three survey tracks during cruise OR1-1164. Mounds were observed on all of the ten survey tracks. Six of the ten survey tracks have a distributed length of mounds larger than 10% of the survey track length, including SV1-1139-VCorer-Dive07-1-SG (52.2%), SV1-1139-VCorer-Dive08-1-SG (65.72%), SV3-1942-ATIS-Dive08-1-SG (34.42%), SV1-1164-TVG-Dive02-1-UU (57.94%), SV1-1164-TVG-Dive03-1-SG (13.79%), and SV1-1164-TVG-Dive04-1-UU (20.59%).

The distributed ratio of mounds on each survey track at site PFZ is listed in Table 5. A total of nine survey tracks were executed at site PFZ; the V-Corer was used to execute two survey tracks during cruise OR1-1139; the ATIS was used to execute three survey tracks during cruise OR3-1942; the TVG was used to execute one survey track during cruise OR1-1164; the FITS was used to execute two survey tracks during cruise OR3-2012A and one survey track dur-

ing cruise OR3-2012B. Mounds were observed on six of the nine survey tracks. Two of the nine survey tracks have a distributed length of mounds larger than 10% of the survey track length, including SV1-1139-VCorer-Dive05-1-SG (10.46%) and SV1-1139-VCorer-Dive06-1-SG (19.32%).

The distributed ratio of mounds on each survey track at site MHV is listed in Table 6. A total of four survey tracks were executed at site MHV; the FITS was used to execute one survey track during cruise OR3-2012A and three survey tracks during cruise OR3-2012B. Mounds were observed on all of the four survey tracks. One of the four survey tracks has a distributed length of mounds larger than 10% of the survey track length, i.e., SV3-2012B-FITS-Dive03-3-UD (48.67%).

The distributed ratio of mounds on each survey track at site FVD-1 is listed in Table 7. A total of two survey tracks were executed using the FITS at site FVD-1 during cruise OR3-2012B. Mounds were observed on both of the survey tracks. Both of the survey tracks have a distributed length of mounds larger than 10% of the survey track length, including SV3-2012B-FITS-Dive04-1-UU (78.29%) and SV3-2012B-FITS-Dive04-2-SU (75.61%).

The distributed ratio of mounds on each survey track at site GLM is listed in Table 8. A total of six survey tracks were executed at site FVD-1; the FITS was used to execute three survey tracks during cruise OR3-2012A and three survey tracks during cruise OR3-2012B. Mounds were observed on three of the six survey tracks. Two of the six survey tracks have a distributed length of mounds larger than 10% of the survey track length, including SV3-2012B-FITS-Dive04-1-UU (78.29%) and SV3-2012B-FITS-Dive04-2-SU (75.61%).

The total length of survey tracks on which mounds were observed at sites YK4-1, PFZ, MHV, FDV-1, and GLM are listed in Table 9. At site YK4-1, the total survey track length is 26.21 km, and the length of survey tracks on which mounds were observed is accumulated as 3.97 km, taking 15.15% of the total survey track length. At site PFZ, the total survey track length is 27.09 km, and the length of survey tracks on which mounds were observed is accumulated as 0.56 km, taking 2.07% of the total survey track length. At site GLM, the total survey track length is 16.3 km, and the length of survey tracks on which mounds were observed is accumulated as 0.93 km, taking 5.71% of the total survey length. At site FDV-1, the total survey track length is 4.22 km, and the length of survey tracks on which mounds were observed is 3.26 km, taking 77.25% of the total survey track length. At site MHV, the total survey track length is 8.87 km, and the length of survey tracks on which mounds were found is 0.75 km, taking 8.46% of the total survey track length.

During cruise OR1-1139 in 2016, the deep-sea winch typically used to operate the V-Corer malfunctioned due to oil leaks. Thus, the viewing system and sensors of the V-Corer were ported to a CTD rosette which was operated

Table 4. Distributed ratios of mounds at site YK4-1.

Survey track	Length of survey track (km)	Distributed length of mounds (km)	Distributed ratio of mounds (%)
SV1-1139-VCorer-Dive04-1-SG	1.07	0.01	1.23
SV1-1139-VCorer-Dive07-1-SG	1.01	0.52	52.20
SV1-1139-VCorer-Dive08-1-SG	1.32	0.86	65.72
SV3-1942-ATIS-Dive02-1-SG	2.27	0.16	6.93
SV3-1942-ATIS-Dive06-1-SG	6.45	0.06	0.96
SV3-1942-ATIS-Dive07-1-SG	8.89	0.13	1.51
SV3-1942-ATIS-Dive08-1-SG	2.24	0.77	34.42
SV1-1164-TVG-Dive02-1-UU	2.33	1.35	57.94
SV1-1164-TVG-Dive03-1-SG	0.29	0.04	13.79
SV1-1164-TVG-Dive04-1-UU	0.34	0.07	20.59

Table 5. Distributed ratios of mounds at site PFZ.

Survey track	Length of survey track (km)	Distributed length of mounds (km)	Distributed ratio of mounds (%)
SV1-1139-VCorer-Dive05-1-SG	0.86	0.09	10.46
SV1-1139-VCorer-Dive06-1-SG	0.79	0.15	19.32
SV3-1942-ATIS-Dive03-1-SG	7.31	0.00	0.00
SV3-1942-ATIS-Dive05-1-SG	5.54	0.00	0.00
SV3-1942-ATIS-Dive06-1-SG	4.30	0.00	0.00
SV1-1164-TVG-Dive01-1-UU	2.41	0.09	3.73
SV3-2012A-FITS-Dive02-1-UD	1.84	0.13	7.07
SV3-2012A-FITS-Dive02-2-UD	2.51	0.07	2.79
SV3-2012B-FITS-Dive01-1-UD	1.53	0.03	1.96

Table 6. Distributed ratios of mounds at site MHV.

Survey track	Length of survey track (km)	Distributed length of mounds (km)	Distributed ratio of mounds (%)
SV3-2012A-FITS-Dive03-1-UD	3.18	0.04	1.26
SV3-2012B-FITS-Dive03-1-UD	1.86	0.01	0.54
SV3-2012B-FITS-Dive03-2-UD	2.70	0.15	5.56
SV3-2012B-FITS-Dive03-3-UD	1.13	0.55	48.67

Table 7. Distributed ratios of mounds at site FVD-1.

Survey track	Length of survey track (km)	Distributed length of mounds (km)	Distributed ratio of mounds (%)
SV3-2012B-FITS-Dive04-1-UU	2.58	2.02	78.29
SV3-2012B-FITS-Dive04-2-SU	1.64	1.24	75.61

Table 8. Distributed ratios of mounds at site GLM.

Survey track	Length of survey track (km)	Distributed length of mounds (km)	Distributed ratio of mounds (%)
SV3-2012A-FITS-Dive01-1-UD	2.01	0.00	0.00
SV3-2012A-FITS-Dive01-2-UD	3.29	0.00	0.00
SV3-2012A-FITS-Dive01-3-UD	2.12	0.18	8.49
SV3-2012B-FITS-Dive02-1-UD	2.37	0.00	0.00
SV3-2012B-FITS-Dive02-2-UD	4.82	0.51	10.58
SV3-2012B-FITS-Dive02-3-UD	1.69	0.24	14.20

Table 9. Distributed ratios of mounds at sites YK4-1, PFZ, MHV, FDV-1, and GLM.

Site	Total length of survey tracks (km)	Total length of survey tracks on which mounds are observed (km)	Distributed ratio of mounds (%)
YK4-1	26.21	3.97	15.15
PFZ	27.09	0.56	2.07
MHV	8.87	0.75	8.46
FDV-1	4.22	3.26	77.25
GLM	16.3	0.93	5.71

through a hydrographic winch. As a result, the V-Corer was used only for seafloor imaging at survey sites YK4-1 and PFZ in 2016. However, before the deep-sea winch malfunctioned during OR1-1139, the V-Corer was used for seafloor sampling at two sites, including A4 and A6 shown in Fig. 21, which are not the primary sites of interest for the CGS seafloor survey project in 2016 and 2017. At site A4, the V-Corer was equipped with ten core tubes and carried out sediment coring one time; seven sediment cores were obtained, leading to a recovery rate of 70% in this coring operation. At site A6, the V-Corer was equipped with twelve core tubes and carried out sediment coring one time; eleven sediment cores were obtained, leading to a recovery rate of about 92% in this coring operation. Additionally, since the V-Corer was not used for the CGS seafloor survey project in 2017, the recovery rate of the V-Corer sampling is not available for year 2017.

Figures 22 and 23 show the comparisons between optical and sonar images obtained on survey track SV3-2012B-FITS-Dive02-2 by the FITS through its downward-looking video camera and MBES, respectively, at site GLM during cruise OR3-2012B. The lower portion of Figs. 22 or 23 consists of four screens, including a wedge screen (upper left), a detection screen (lower left), a side scan screen (upper right), and a snippets screen (lower right), which are provided by the Odom Sonar User Interface of Teledyne Reson. The wedge screen shows the bathymetric data as a complete swath illuminated by a single transmitted ping with a quality-based multibeam data color mode; the history of the bathymetric data is also displayed in the wedge screen. The detect screen shows the bathymetric data of a single swath with a quality-based multibeam data color mode. The side scan screen shows an image of the seafloor; each sonar ping is used to generate a line of data, and each line of data contain a series of amplitudes representing the returned signals versus time or range. The snippets screen shows the backscatter data in a waterfall display; a snippets data sample contains corrected backscatter data from the features on the seafloor illuminated by a single sonar ping; each snippets data packet contains pertinent information such as the time stamp, sequential ping number, sample rate, sound velocity, and operator settings such as the power, gain, absorption,

and range scale. As shown in Figs. 22 and 23, the mounds observed in the optical images can also be identified in the sonar images displaying in the wedge screen, sonar screen, and snippets screen. The comparison results suggest that the optical images obtained by the IUT deep-towed vehicles can be solid visual evidence for high resolution geophysical data obtained by deep-towed sonar systems.

In addition, Fig. 24 shows the comparison between the estimated area of mounds at site PFZ and the side scan sonar image obtained from (Hsu 2017). Likewise, Fig. 25 shows the comparison between the estimated area of mounds at site GLM and the side scan sonar image obtained from (Hsu 2017) as well. Based on the comparison results shown in Figs. 24 and 25, the areas of mounds estimated using optical images at sites PFZ and GLM match the areas with rough seafloor characteristics in the side scan sonar images.

5. CONCLUSION

In 2016 and 2017, the IUT performed seafloor imaging and sampling for mineral resource investigation at five survey sites including YK4-1, PFZ, MHV, FDV-1, and GLM, in the south Okinawa Trough off northeastern Taiwan through five survey cruises, as listed in Table 10. The deep-towed vehicles utilized for the seafloor video surveys and sampling include the ATIS, V-Corer, TVG, and FITS, which are all developed by the IUT.

Based on the survey results obtained in 2016 and 2017, the physical and biological features of the seafloor at the five survey sites are summarized as follows:

- (1) Site YK4-1: Hydrothermal activities and squat lobsters are observed on some mounds. Samples of deep-sea mussels, squat lobsters, mound pieces, and sediments are collected through the TVG.
- (2) Site PFZ: Mounds are found to be distributed within a radius of 500 m from the center of site PFZ. Clusters of squat lobsters and deep-sea mussels are observed on some mounds. Parts of the seafloor are covered possibly by carbon dioxide hydrates. Some mounds are found to have metallic/crystal reflections. Mound samples with such reflections are collected through the TVG.
- (3) Site MHV: Empty mussel shells, deep-sea mussels, and

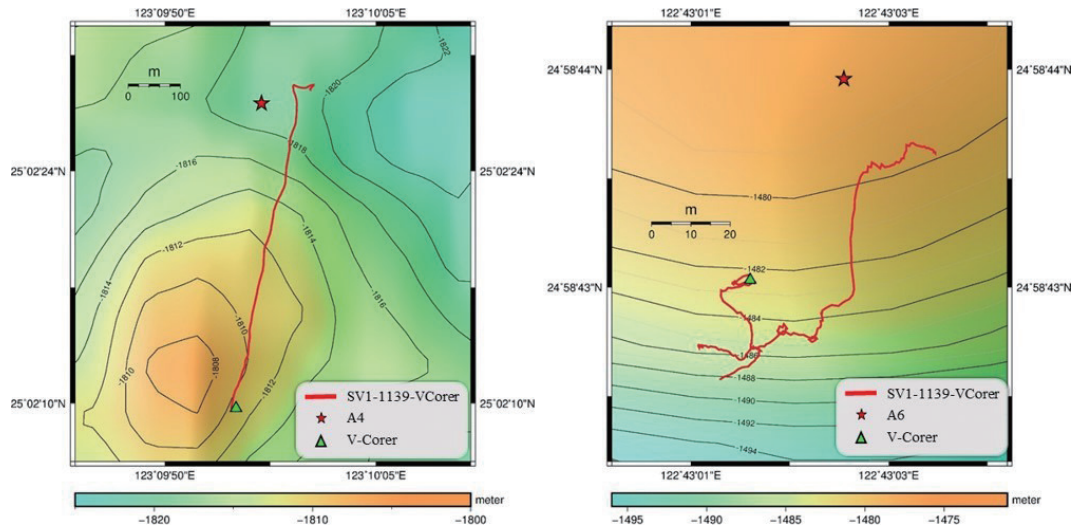


Fig. 21. Survey sites A4 (left) and A6 (right) where the V-Corer was used for seafloor sampling in 2016.

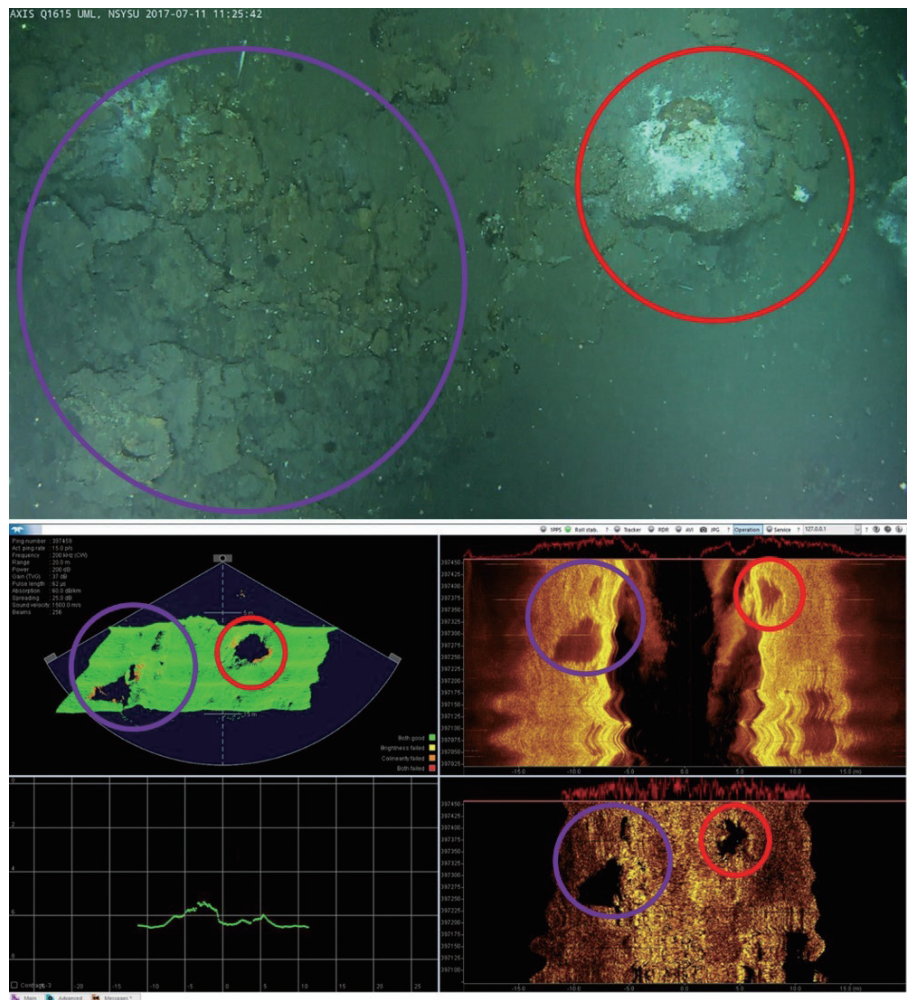


Fig. 22. Comparison #1 between optical and sonar images obtained by the FITS at site GLM.

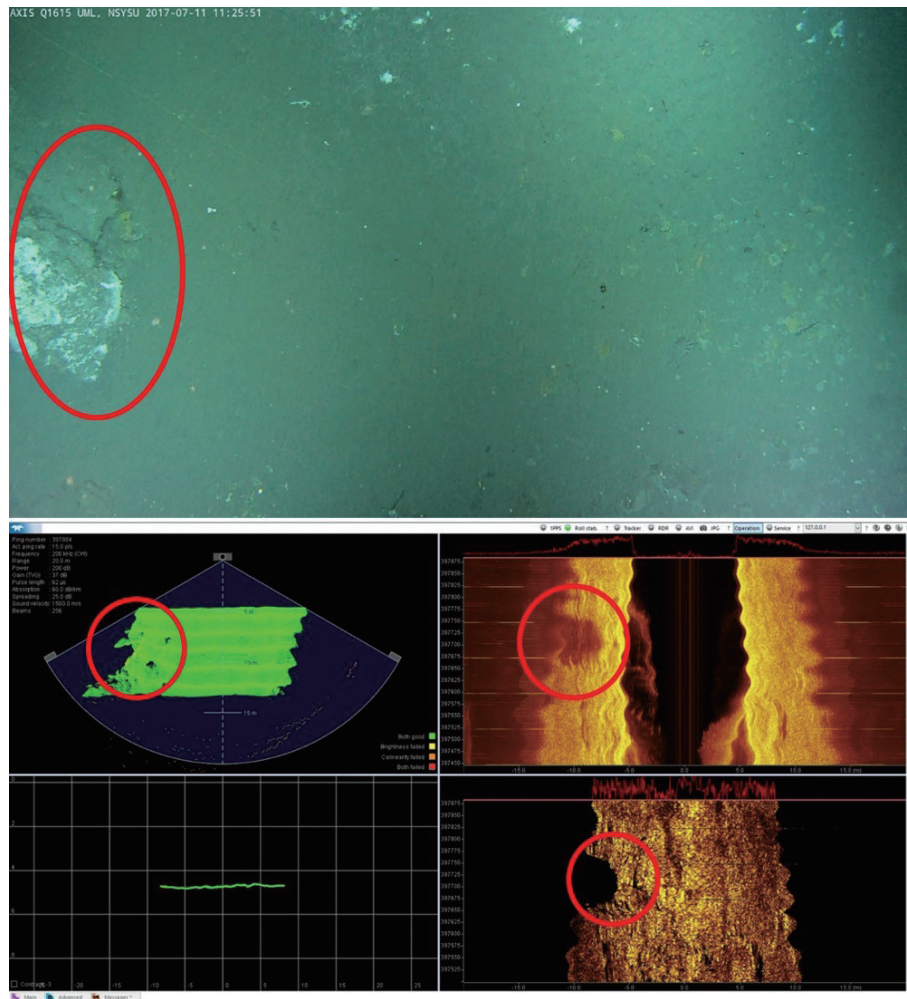


Fig. 23. Comparison #2 between optical and sonar images obtained by the FITS at site GLM.

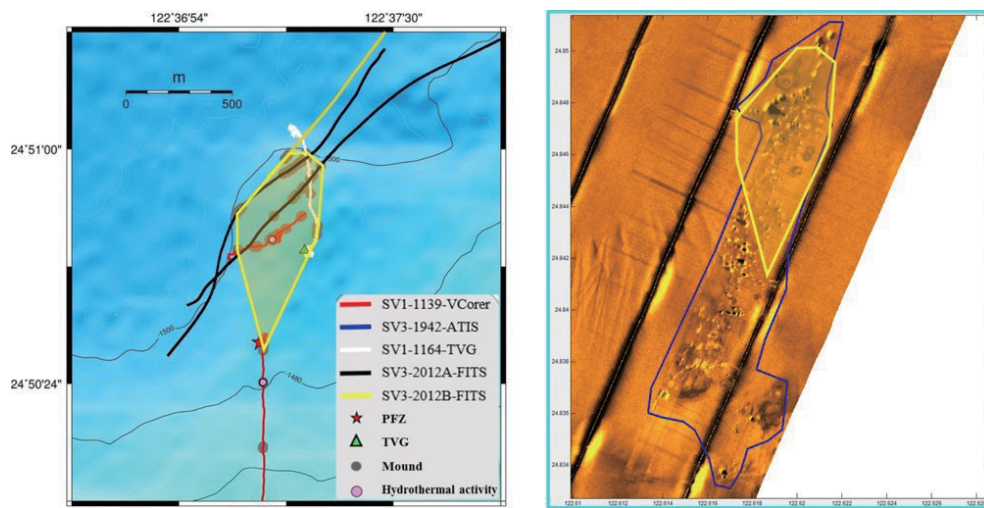


Fig. 24. Comparison between estimated mound area at site PFZ and side scan sonar image from (Hsu 2017).

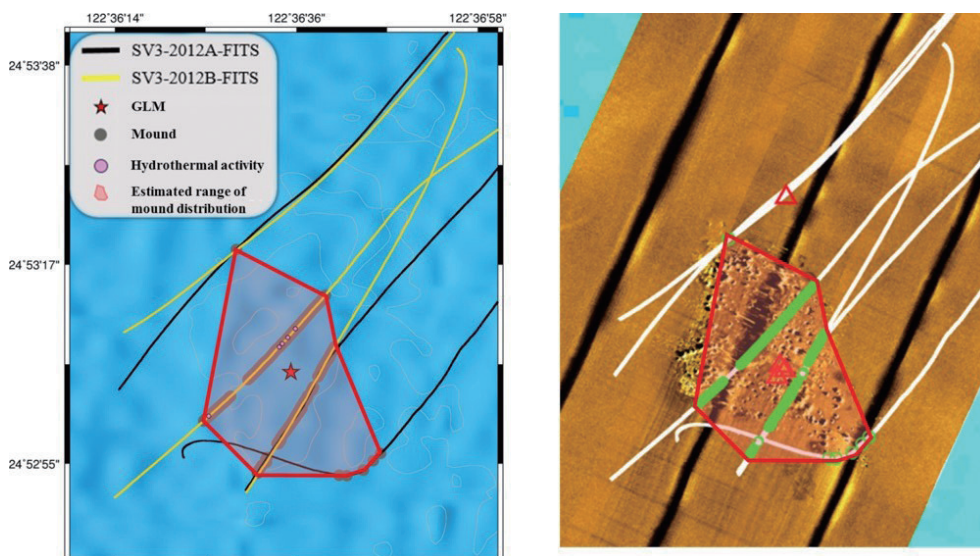


Fig. 25. Comparison between estimated mound area at site GLM and side scan sonar image from (Hsu 2017).

Table 10. Seafloor survey cruises conducted by the IUT in 2016 and 2017.

Date	Cruise	Vehicle	Survey site				
			YK4-1	PFZ	MHV	FDV-1	GLM
June 2016	OR1-1139	V-Corer	√	√			
July 2017	OR3-1942	ATIS	√	√			
May 2017	OR1-1164	TVG	√	√			
July 2017	OR3-2012A	FITS		√	√		√
	OR3-2012B	FITS		√	√	√	√
Coverage (km)			26.21	27.09	8.87	4.22	16.30

squat lobsters are found on a few mounds located in the flat area on the east side of the volcano. Deep-sea mussels, squat lobsters, and hydrothermal activities gradually appear on the mounds in the foothill area on the south side of the volcano.

- (4) Site FDV-1: Mounds are found to be widely distributed, and empty mussel shells are observed on some mounds at site FDV-1.
- (5) Site GLM: Lots of mounds are observed within a radius of 500 m from the center of site GLM. But squat lobsters and deep-sea mussels are found only on a few mounds. Five active hydrothermal chimneys are observed at site GLM.

The seafloor survey results, including the video data and the samples of animals, sediments, and mounds, have been provided to different scientific teams for conducting research on marine geophysics, marine geology, marine geochemistry, and marine ecology. The video data can be cross-checked and used as the supporting evidence for the analysis results from the scientific researchers.

Acknowledgements This research is supported by: (1) the Central Geological Survey, the Ministry of Economic Affairs (Taiwan), under grants 105-5226904000-08-03, 106-5226904000-05-03, 107-5226904000-05-03, B10650, and B10742; (2) the Ministry of Science and Technology (Taiwan), under grants MOST 106-3113-M-110-001, MOST 107-3113-M-110-001, MOST 107-2218-E-110-005, MOST 107-2218-E-110-006, MOST 108-2218-E-110-003, and MOST 108-2218-E-110-004.

REFERENCES

- Chen, H.-H., 2017: Geological Investigation of Mineral Resource Potential in the Offshore Northeastern Taiwan: Video Surveys and Sampling of Seafloor Mineral Deposits (2/4), Report of Central Geological Survey, 106-14-B, 156 pp. (in Chinese with English abstract)
- Chen, H.-H., C.-C. Wang, Y.-C. Chou, P.-C. Hsueh, Y.-H. Lin, and J.-M. Lin, 2017: Deep-towed vehicles for seafloor imaging and sampling off Taiwan. OCEANS

- 2017 - Aberdeen, IEEE, Aberdeen, UK, 7 pp, doi: 10.1109/OCEANSE.2017.8084575. [[Link](#)]
- Chen, S.-C., S.-K. Hsu, C.-H. Tsai, C.-Y. Ku, Y.-C. Yeh, and Y. Wang, 2010: Gas seepage, pockmarks and mud volcanoes in the near shore of SW Taiwan. *Mar. Geophys. Res.*, **31**, 133-147, doi: 10.1007/s11001-010-9097-6. [[Link](#)]
- Doo, W.-B., S.-K. Hsu, H.-F. Wang, Y.-S. Huang, C.-H. Tsai, C.-L. Lo, S.-S. Lin, C.-W. Liang, and Y.-J. Lin, 2019: A deep-towed magnetic survey in the southern Okinawa Trough: Implications for hydrothermal system detection. *Terr. Atmos. Ocean. Sci.*, **30**, 675-683, doi: 10.3319/TAO.2019.02.15.01. [[Link](#)]
- Fornari, D. J., 2003: A new deep-sea towed digital camera and multi-rock coring system. *Eos, Trans. AGU*, **84**, 69-73, doi: 10.1029/2003EO080001. [[Link](#)]
- Hsu, H.-H., L.-F. Lin, C.-S. Liu, J.-H. Chang, W.-Z. Liao, T.-T. Chen, K.-H. Chao, S.-L. Lin, H.-S. Hsieh, and S.-C. Chen, 2019: Pseudo-3D seismic imaging of Geolin Mounds hydrothermal field in the Southern Okinawa Trough offshore NE Taiwan. *Terr. Atmos. Ocean. Sci.*, **30**, 705-716, doi: 10.3319/TAO.2019.03.14.02. [[Link](#)]
- Hsu, S.-K., 2016: Geological Investigation of Mineral Resource Potential in the Offshore Northeastern Taiwan: High-resolution Sonar and Magnetic Surveys (1/4), Report of Central Geological Survey, 105-13, 238 pp. (in Chinese with English abstract)
- Hsu, S.-K., 2017: Geological Investigation of Mineral Resource Potential in the Offshore Northeastern Taiwan: High-resolution Sonar and Magnetic Surveys (2/4), Report of Central Geological Survey, 106-13, 237 pp. (in Chinese with English abstract)
- Lin, J.-Y., W.-N. Wu, C.-C. Su, C.-H. Tsai, H.-H. Sun, Y.-F. Chen, S.-J. Chin, and Y.-C. Lin, 2019a: Spatial and temporal distribution of low frequency volcanic earthquakes in the southern Okinawa Trough back-arc basin. *Terr. Atmos. Ocean. Sci.*, **30**, 621-631, doi: 10.3319/TAO.2018.12.24.01. [[Link](#)]
- Lin, S., W.-C. Hsieh, Y. C. Lim, T.-F. Yang, C.-S. Liu, and Y. Wang, 2006: Methane migration and its influence on sulfate reduction in the Good Weather Ridge region, South China Sea continental margin sediments. *Terr. Atmos. Ocean. Sci.*, **17**, 883-902, doi: 10.3319/TAO.2006.17.4.883(GH). [[Link](#)]
- Lin, Y.-S., H.-T. Lin, B.-S. Wang, S.-F. Wu, P.-L. Wang, C.-L. Wei, H.-F. Lee, T. Lan, W.-J. Huang, S.-C. Chen, Y. Wang, and C.-C. Su, 2019b: Early diagenesis and carbon remineralization in young rift sediment of the Southern Okinawa Trough. *Terr. Atmos. Ocean. Sci.*, **30**, 633-647, doi: 10.3319/TAO.2019.01.10.01. [[Link](#)]
- Liu, C.-S., 2016: Geological Investigation of Mineral Resource Potential in the Offshore Northeastern Taiwan: Seismic and Heat Flow Surveys (Master Project) (1/4), Report of Central Geological Survey, 105-12, 136 pp. (in Chinese with English abstract)
- Liu, C.-S., 2017: Geological Investigation of Mineral Resource Potential in the Offshore Northeastern Taiwan: Seismic and Heat Flow Surveys (Master Project) (2/4), Report of Central Geological Survey, 106-12, 133 pp. (in Chinese with English abstract)
- Su, C.-C., 2016: Geological Investigation of Mineral Resource Potential in the Offshore Northeastern Taiwan: Master Project and Geochemical Investigation (1/4), Report of Central Geological Survey, 105-14-A, 204 pp. (in Chinese with English abstract)
- Su, C.-C., 2017: Geological Investigation of Mineral Resource Potential in the Offshore Northeastern Taiwan: Geochemical Investigation and Sea Floor Imaging (Master Project) (2/4), Report of Central Geological Survey, 106-14, 80 pp. (in Chinese with English abstract)
- Tsai, C.-H., S.-K. Hsu, Y.-F. Chen, H.-S. Lin, S.-Y. Wang, S.-C. Chen, C.-W. Liang, and Y.-Y. Cho, 2019: Gas plumes and near-seafloor bottom current speeds of the southernmost Okinawa Trough determined from echosounders. *Terr. Atmos. Ocean. Sci.*, **30**, 649-674, doi: 10.3319/TAO.2019.07.07.01. [[Link](#)]
- Wang, C.-C., 2016: Geological Investigation of Mineral Resource Potential in the Offshore Northeastern Taiwan: Video Surveys and Sampling of Seafloor Mineral Deposits (1/4), Report of Central Geological Survey, 105-14-B, 70 pp. (in Chinese with English abstract)
- Wang, C.-C., H.-H. Chen, S.-C. Chen, and Y. Wang, 2015: An introduction to the national energy program — Gas hydrate exploration in Taiwan. OCEANS 2015 - Genova, IEEE, Genova, Italy, 6 pp, doi: 10.1109/OCEANS-Genova.2015.7271667. [[Link](#)]
- Wu, T.-W., W.-C. Chi, Y.-S. Lin, and S.-C. Chen, 2019: Temperature as a tracer for fluid movement at hydrothermal sites near the Yonaguni Knoll IV, Okinawa Trough. *Terr. Atmos. Ocean. Sci.*, **30**, 695-704, doi: 10.3319/TAO.2019.01.10.02. [[Link](#)]